ASSESSMENT OF POWER CONSUMPTION OF HELICOPTER FLIGHT CONTROL SYSTEMS WITHOUT SWASHPLATE

NEUHEUSER, Tom
Hamburg University of Technology
Institute for Aircraft Systems Engineering
Neßpriel 5, 21129 Hamburg, Germany
Phone: +49 (0)40 / 428 788-211
Fax: +49 (0)40 / 428 788-270
E-Mail: neuheuser@tuhh.de

CARL, Udo
Hamburg University of Technology
Institute for Aircraft Systems Engineering
Neßpriel 5, 21129 Hamburg, Germany
Phone: +49 (0)40 / 428 788-201
Fax: +49 (0)40 / 428 788-270
E-Mail: carl@tuhh.de

ABSTRACT
Nowadays helicopter flight control in the most common configurations is realized by collective and cyclic variation of the angle of attack of each rotor blade. The collective blade control pitches the rotor blades to equal angles of attack around their longitudinal axis, changing the rotor thrust at constant rotor speed. Yaw and roll control is realized via cyclic blade motion by changing the angle of attack of every rotor blade locally and periodically during one revolution. Although fly-by-wire and fly-by-light technologies slowly have found entry into helicopter flight control systems in the last years, complex mechanical systems are state-of-the-art to transfer all required control signals and forces from the fuselage into the rotating main rotor system. By Individual Blade Control (IBC) in higher harmonic modes and with additional actuators in the rotating system, fuselage vibrationsand radiated noise can be reduced and as well other IBC effects. This technology is subject of intensive research work [1].
The intention of the research project INHUS ("Innovative Steuerungskonzepte für Hubschrauber") is the identification of a combined actuation system for primary flight control and IBC, which corresponds to the essential requirements of light weight, low control power consumption and high reliability. Therefore, a wide variety of technologies will be evaluated in terms of aforementioned requirements, uneffected by known flight control implementations in helicopters.
The content of this paper is the comparison of the required power of different hydraulic and electric actuation systems, designed on the basis of specification data of a 20 tons–helicopter during several steady flight conditions.

KEYWORDS
electric control, diplacement control, helicopter, valve control, helicopter flight control actuation system, power.

1 INTRODUCTION
Figure 1 shows a conventional flight control actuation system for helicopters. On one hand the pitch angle ϑ_b at each root of a rotor blade results from the collective and cyclic blade control of the primary flight control. They were realized by a pitch link between the rotating part of the swashplate and the root of the blade. If the swashplate is slantd forward or to the side, the pitch angle of each rotor blade changes during a revolution (cyclic blade control). If the swash plate moves up or down, the pitch angle of all rotor blades changes at the same time (collective blade control). Because of the high aerodynamic torques $M_{L,b}$ that are encountered by the rotor blades, hydraulic actuators are installed in the control system to assist the pilot moving the swashplate [6]. On the other hand the pitch angle ϑ_b results from the high frequency signals of the IBC-control. They are realized by hydraulik actuators integrated into the pitch link. The main rotor is driven by a shaft with constant speed Ω.

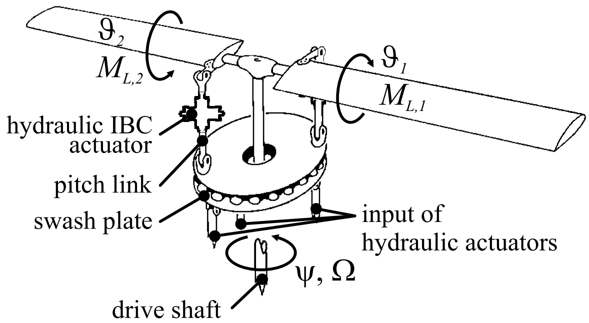

Fig. 1: conventional helicopter flight control system

It appears attractive to integrate primary flight control functions and IBC of an helicopter into one actuation system without swashplate, located at each blade in the rotating system, to reduce complexity and weight and to enhance reliability, availability and maintainability of helicopter flight control systems.
With the selection of an adequate actuation system, control power consumption is a fundamental criterion. Therefore the required power at each blade and thus of the whole rotor system, based on measurement data in different steady flight conditions, was determined. Subsequently, the losses and the control power consumption of two hydraulic and one electrical actuation system were determined respectively, based on specification data of a 20 tons–helicopter, in an inverse calculation in identical flight conditions.

2 POWER REQUIREMENTS
In this section, first the required power of the whole rotor system is computed as a base for later comparison of control power consumption of different actuation systems.
From tests in steady flight conditions with airspeeds

(1) $\quad v \in \{90, 130\}$ kt

and orders

(2) $\quad n \in \{3,5,7\}$ [–]

of higher harmonic IBC-signals the state variables of pitch angle $\vartheta_b(t)$ and load $M_L(t)$ are available. Additionally, various phase shifts and amplitudes of IBC–harmonics are conceivable, but for demonstration purposes, they are set to a constant value in this paper. From this measurement data the required power at one single blade can be calculated with

(3) $\quad P_b(t) = \dot{\vartheta}_b(t) \cdot M_{L,b}(t).$

A fundamental difference between various actuation systems is their potential to transfer power between actuators of different blades, which work in motor-mode or in generator-mode periodically. In an actuation system with cross supply power is transfered from actuators in generator-mode to other actuators in motor-mode. This has to be considered in the determination of the control power consumption of the whole rotor system. Therefore, two cases are considered below.

Actuation system with cross supply. The required power of the whole rotor system is identified from the required power at each single blade (see eq. (3)) with

(4) $$P_{wcs}(t) = \sum_{b=1}^{k} P_b(t).$$

The mean value of the required power during one revolution of the rotor system can be written as

(5) $$\bar{P}_{wcs} = \frac{\Omega}{2 \cdot \pi} \cdot \int_0^{\frac{2\cdot\pi}{\Omega}} P_{wcs}(t)\, dt.$$

The left ordinate in figure 2 shows the mean values $\bar{P}_{wcs}$ of the required power of the whole rotor system in above mentioned steady flight conditions. The right ordinate shows additionally the difference

(6) $$\Delta\bar{P}_{wcs} = \bar{P}_{wcs}\,|_{\text{with IBC}} \quad - \quad \bar{P}_{wcs}\,|_{\text{without IBC}}$$

between the mean required power in identical flight conditions with and without IBC.
It can be oberserved, that $\bar{P}_{wcs}$ increases with rising airspeed v. Also it can be stated that in most flight conditions with IBC more control power is required, but in some conditions little less control power is observed. The results vary with the phase shift neglected here, but they are in the same range. Further systematics in the results are not observable.
All values in this paper are scaled with maximum occured power P_N.

Actuation system without cross supply. It depends on the individual actuation system, what happens with generated power at the root of a single blade. However, in the actuation systems without cross supply, considered in chapter 3 in this paper, this condition requires a power input of the actuation system. So the required power of a single blade is given with

(7) $$P_{wocs}(t) = \sum_{b=1}^{k} |P_b(t)|.$$

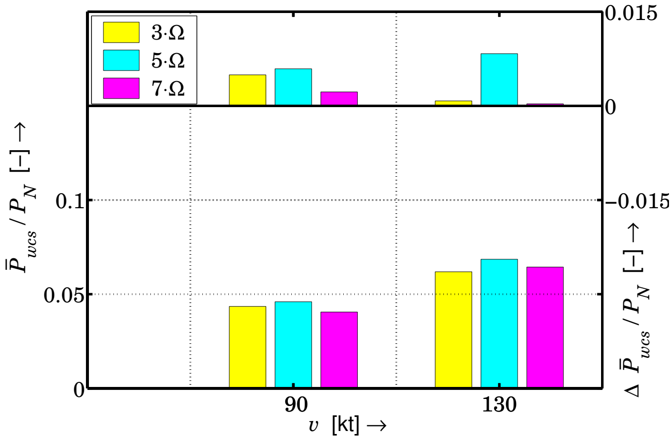

Fig. 2: required power $\bar{P}_{wcs}$ with cross supply

Identical to eq. (5) the mean value of the required power during one revolution of the rotor system $\bar{P}_{wocs}$ can be calculated. Figure 3 shows the mean values $\bar{P}_{wocs}$ of the required power of the whole rotor system in the left ordinate in identical flight conditions shown in figure 2. The right ordinate again shows the difference $\Delta\bar{P}_{wocs}$ to the mean required power in identical flight conditions without IBC.

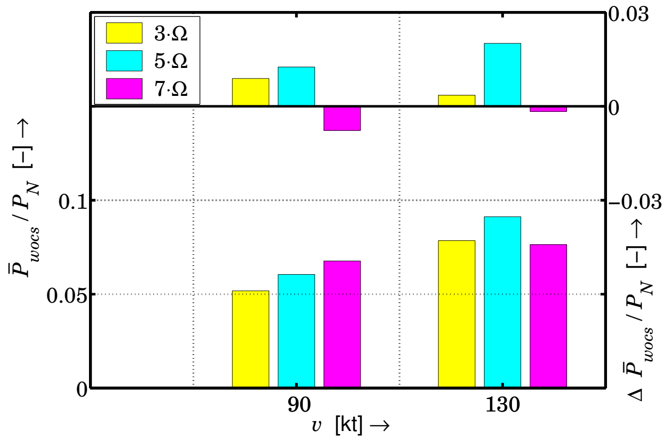

Fig. 3: required power $\bar{P}_{wocs}$ without cross supply

Generally, a higher power requirement can be determined here in comparison with the results from figure 2, since no actuator in motor-mode can be supplied from actuators in generator-mode. Further systematic differences to the results in figure 2 can not be observed.

3 HYDRAULIC VALVE CONTROL

The design of this actuation system for a single rotor blade in principle is depicted in figure 4.

A linear hydraulic cylinder is connected to the rotor blade by a lever with length l. The commanded pitch $\vartheta_{c,b}$ is controlled with flows $Q_{A,b} = -Q_{B,b}$ to the cylinder by a 4/3-servovalve, whereas the pressures $p_{A,b}$ and $p_{B,b}$ results due to the effective piston area A_K and the loads $M_{L,b}$ and $F_{L,b}$ respectively. The valve is connected to a constant pressure network, which delivers

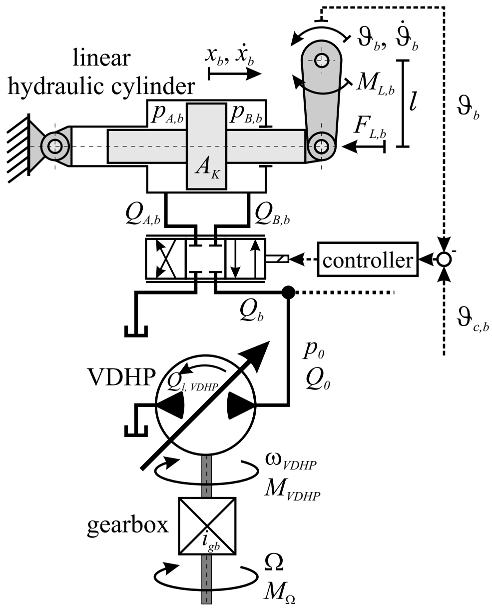

Fig. 4: hydraulic valve control in principle

the required flow

(8) $\quad Q_b(t) = |Q_{A,b}(t)| = |Q_{B,b}(t)|$

to the valve. Thus, the actuator also needs a power input, if the state at the root of the blade is in generator-mode. So no cross supply is possible. The constant pressure p_0 is assured by a pressure controlled variable displacement hydraulic pump (VDHP). This is an axial piston unit, driven from the main rotor shaft. Due to the constant rotor speed Ω, the pump speed ω_{VDHP} can be adjusted by a gearbox with ratio i_{gb}. All components in this system were designed according to specification data of a 20 tons–helicopter with IBC.

The losses in the servovalve in this system architecture are immanent, because the valve produces the required flows $Q_{A,b}$ and $Q_{B,b}$ from the constant pressure net by a variable orifice. Thus, the power

$$(9) \quad P_{SV,b}(t) = p_0 \cdot Q_b(t) = \underbrace{(p_{A,b}(t) - p_{B,b}(t)) \cdot Q_b(t)}_{\text{active power}} \ldots$$
$$\ldots + \underbrace{[p_0 - p_{A,b}(t) + p_{B,b}(t)] \cdot Q_b(t)}_{\text{power loss} P_{l,SV,b}(t)}$$

is transfered to each servovalve. Thus, the power $P_{l,SV,b}(t)$, described in eq. (9), is always lost at the servovalve.

The losses $P_{l,VDHP}$ in the VDHP can be basically divided into volumetric losses and hydraulic-mechanical losses. A detailed theoretical description of the losses of this pump type is given in [4]. The losses of the pump with respect to the specifications are described in [3].

The ratio i_{gb}, in the way it is necessary here, has to be realized in a three step spur gear. The efficiencies $\eta_{gb}(t)$ results from estimations in [2].

Finally, the control power consumption of the whole rotor system can be described with

$$(10) \quad P_{VC}(t) = \left(\sum_{b=1}^{k} |P_{SV,b}(t)| + P_{l,VDHP}(t) \right) \cdot \frac{1}{\eta_{gb}(t)}.$$

According to the definitions in eq. (5) the mean values $\bar{P}_{VC}$ of the required power with IBC during one revolution of the rotor system is depicted in the left ordinate in figure 5 in identical flight conditions as in chapter 2. No further comparisons to flight conditions without IBC are made, because the design of all components depends on the capability of the control system to provide IBC. Thus higher losses results from flight conditions without IBC with the system design accomplished in this paper. Additionally the overall efficiency

$$(11) \quad \eta_{VC} = \frac{\bar{P}_{wocs}}{\bar{P}_{VC}} \cdot 100 \quad [\%]$$

is noted.

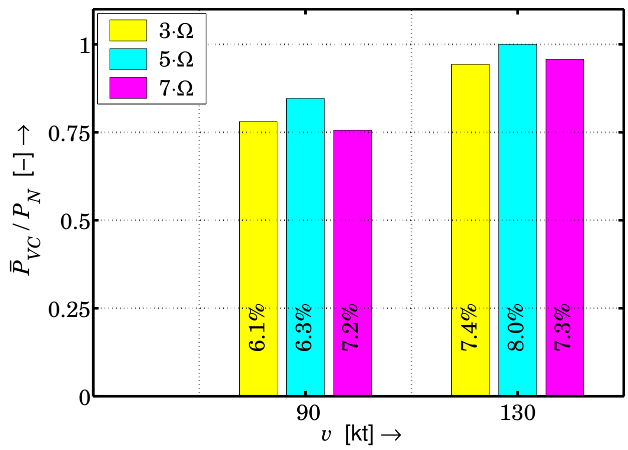

Fig. 5: power consumption $\bar{P}_{VC}$ of hydraulic valve control

Similar to the results in chapter 2, the mean control power consumption $\bar{P}_{VC}$ increases with rising airspeed v. Futher it can be stated that by IBC only little more or even less control power consumption occurs.

The low efficiencies $\eta_{VC} \approx 6\ldots8$ % result from the specification, which postulating a reserve for the rotating speed at the root of a rotor blade $\dot{\vartheta}_b$ and loads $M_{L,b}$ for manouever demands. These maximum speeds and loads were not achieved in the steady flight conditions considered here. Hence, high power losses $P_{l,SV,b}$ can be oberserved, as given in eq.(9).

4 HYDRAULIC DISPLACEMENT CONTROL

Figure 6 depicts the design principle of the actuation system with hydraulic displacement control for a single rotor blade.

Similar to the system described in chapter 3 a linear hydraulic cylinder is connected to the rotor blade by a lever with length l. In this concept the commanded pitch $\vartheta_{c,b}$ is controlled with flows $Q_{A,b} = -Q_{B,b}$ to the cylinder by VDHP. The pressures $p_{A,b}$ and $p_{B,b}$ results due to the effective piston area A_K and the loads $M_{L,b}$ and $F_{L,b}$ respectively. The VDHP is driven with a constant speed ω_{VDHP} through a gearbox with the ratio i_{gb} by the main shaft with the speed Ω. Also, all components in this system were designed according to specification data of a 20 tons–helicopter with IBC.

The VDHP can operate as a motor during generator states at the root of a rotor blade. Therefore, this actuation system allows a power cross supply between single actuators by means of the

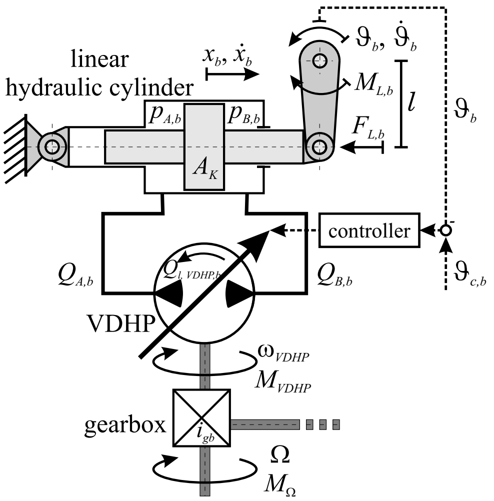

Fig. 6: hydraulic displacement control in principle

mechanical connection between all actuators via shafts and the gearbox.
The losses $P_{l,VDHP,b}$ in the VDHP and the efficiency $\eta_{gb}(t)$ of the gearbox were mentioned in chapter 3 and can also be taken from [2, 3, 4].
Hence, the control power consumption of the whole rotor system is given with

$$(12)\quad P_{DC}(t) = \sum_{b=1}^{k} (M_{L,b}(t) \cdot \dot{\vartheta}_b(t) + P_{l,VDHP,b}(t)) \cdot \frac{1}{\eta_{gb}(t)}.$$

Similar to figure 5 the mean values $\bar{P}_{DC}$ of the required power during one revolution of the displacement controlled rotor system is shown in figure 7. According to eq. (11) the efficiencies η_{DC} relating to the mean required power $\bar{P}_{wcs}$ with cross supply are noted.

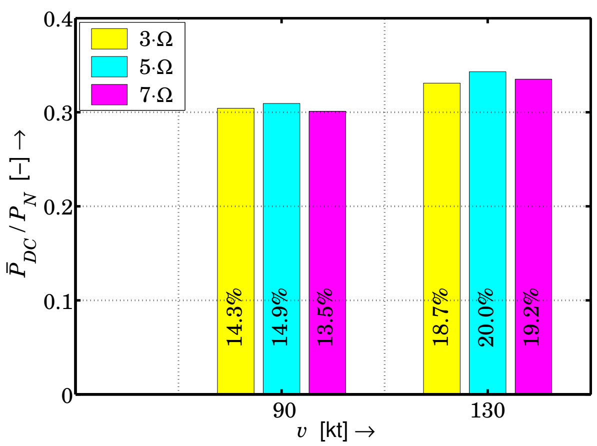

Fig. 7: power consumption $\bar{P}_{DC}$ of hydraulic displacement control

In general, higher efficiencies $\eta_{DC} \approx 14\ldots20$ % in comparison to the efficiencies η_{VC} of the hydraulic valve control can be observed. The main reason for this is, that no immanent losses occur at a valve . Further, no systematic differences to the results in chapter 3 can be determined.

5 ELECTRIC CONTROL

The architecture of an electric controlled actuation system with brushless DC-Motor for a single rotor blade is shown in principle in figure 8.

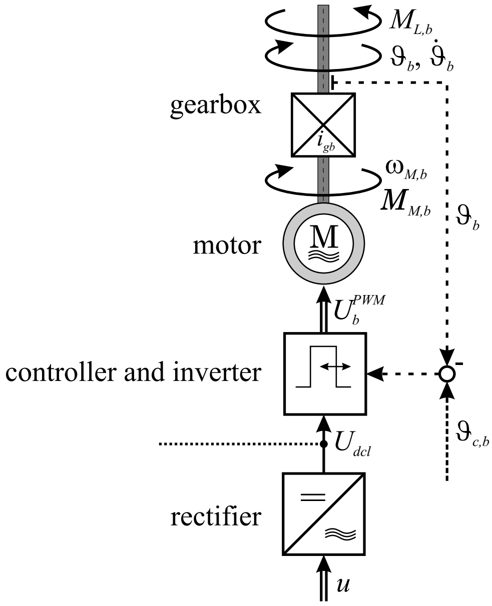

Fig. 8: electric control in principle

The axis of the rotor blade is connected directly to the output of a gearbox with ratio i_{gb}, transforming the rotation speed $\dot{\vartheta}_b$ and the load $M_{L,b}$ at the root of a rotor blade to the speed $\omega_{M,b}$ and load $M_{M,b}$ at the output shaft of the brushless DC-Motor. Additionally, the intertia J_M of the motor and J_{gb} of the gearbox are considered in the torque

$$(13)\quad M_{J,b}(t) = \ddot{\vartheta}_b(t) \cdot (J_M + J_{gb})$$

since frequently changes in the direction of rotation of the motor and gearbox are required.
The motor is energized by a converter, which controls the commanded pitch $\vartheta_{c,b}$. The converters of all motors are energized by an intermediate direct current link. Thus, a power cross supply between motors in motor-mode and generator-mode via the direct current link is possible. A rectifier unit supplies the intermediate direct current link. Also, in this system all components are designed according to specification data of a 20 tons–helicopter with IBC.
The efficiencies η_{gb} are mentioned in the chapters 3 and 4 above and are estimated from [2]. The losses of the motor are estimated by measurements, which were done with a motor of same type but from a different power class. These losses can be intergrated to $\bar{P}_{l,M,b}$ with the losses of the rectifier, described in detail in [5, 7].
The control power consumption of the whole rotor system is given with

(14)

$$P_{EC}(t) = \sum_{b=1}^{k} \left((M_{L,b}(t) + M_{J,b}(t)) \cdot \eta_{gb}(t) \cdot \dot{\vartheta}_b(t) \cdot + P_{l,M,b}(t) \right).$$

The mean control power consumption during one revolution

$\bar{P}_{EC}$ is calculated identically to eq. (5) and are depicted in figure 9.

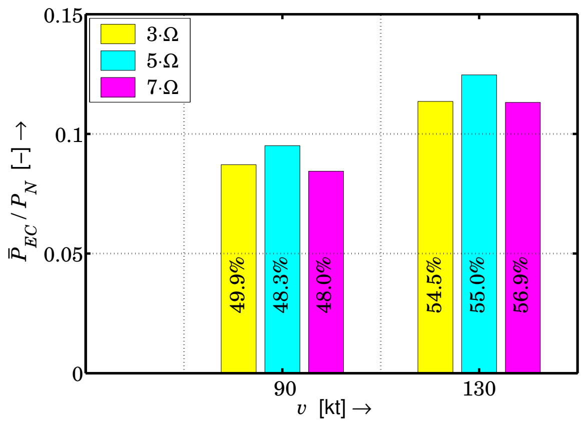

Fig. 9: power consumption $\bar{P}_{EC}$ of electric control

In comparison to the efficiencies η_{VC} of the hydraulic valve control and η_{DC} of the hydraulic displacement control the efficiencies $\eta_{EC} \approx 48\ldots57$ % are the highest. The main reason for this is, that again no immanent system losses occur in this system architecture. Further, the losses in a brushless DC-Motor are comparatively small, if the operating point during steady flight conditions is far away from the nominal operating point.

6 CONCLUSION

The paper presents two hydraulic and one electric actuation system, located at each blade. These systems integrate helicopter flight control system without swashplate and IBC. The required control power at a single rotor blade was calculated from measurement data in different steady flight conditions. Based on this, the required control power of the whole rotor system, taking into account the possibility to transfer power from an actuator in motor-mode to another actuator in generator-mode, was computed.

Each system was designed by specifications of a 20 tons–helicopter. The power losses and efficiencies were estimated as a basis for the calculation of the control power consumption and the overall efficiency of each actuation system. The control power consumption of the hydraulic valve control is comparatively high because of the immanent system losses in the servovlave. A lower control power consumption was determined by the hydraulic displacement control. The highest efficiency and lowest control power consumption was observed with the electric control.

Further criterions like mass, reliability, controllability, redundancy capability plays a role in the selection of an applicable actuation system. They will be included in future work of this research project. Variants of the actuation systems introduced here are conceivable and will be analyzed as well.

REFERENCES

[1] ARNOLD, U. & FÜRST, D.: *Closed Loop IBC Results from Recent CH-53G Flight Tests*. 30th European Rotorcraft Forum, Marseilles, France, 2004.

[2] DECKER, K.-H.: *Maschinenelemente – Gestaltung und Berechnung*. Hanser, München, 1995.

[3] EATON INC. (EDT.): *Fluid Power Division, Inline Pumps, Description Summary SE–103E*. 1995.

[4] IVANTYSYN, J. & IVANTYSYNOVA, M.: *Hydrostatic Pumps and Motors*. Tech Books International, New-Dehli, India, 2003.

[5] MURPHY, J. & TURNBULL, F.: *Power Electronic Control of AC Motors*. Pergamon Press, Oxford, England, 1993.

[6] PALLETT, E. & COYLE, S.: *Automatic Flight Control*. Blackwell Scientific Publications, Oxford, England, 1988.

[7] RAMSHAW, R. S.: *Power Electronics Semiconductor Switches*. Chapmann & Hall, London, England, 1993.

NOTATION

Functions and Scalars

A	m^2	area
ϑ	rad	pitch
$\dot{\vartheta}$	rad/s	rotating speed at root of rotor blade
φ	rad	phaseshift of IBC–harmonic
ψ	rad	azimuth angle of main rotor
F	N	force
k	-	number of blades
M	Nm	torque
P	W	power
t	s	time
v	kt	airspeed
Ω	rad/s	rotating speed of main rotor

Indices

b	relating to rotorblade b
DC	displacement control
dcl	direct current link
EC	electric control
gb	gearbox
K	piston, (*ger.*) Kolben
L	load
l	loss
M	motor
N	scale factor
SV	servovalve
VC	valve control
$VDHP$	**V**ariable **D**isplacement **H**ydraulic **P**ump)
$wocs$	**w**ith**o**ut **c**ross **s**upply
wcs	**w**ith **c**ross **s**upply

ACKNOWLEDGEMENT

The research project INHUS (”Innovative Steuerungskonzepte für Hubschrauber”) is funded by the BUNDESMINISTERIUM FÜR WIRTSCHAFT UND ARBEIT and is accomplished in cooperation between ZF LUFFTAHRTTECHNIK GMBH, GERMAN AEROSPACE CENTER (Deutsches Institut für Luft und Raumfahrt, DLR) and BRAUNSCHWEIG UNIVERSITY OF TECHNOLOGY